Defence Science Journal, Vol. 73, No. 3, May 2023, pp. 362-373, DOI : 10.14429/dsj.73.18456

Ethernet Over Coaxial (EoC) Cable Telemetry Over High Voltage DC and High Power AC for Airborne Sonar Applications

Manoj G.[#,*], R. Ramesh[$] and Sona O. Kundukulam[$]

[#]*Cochin University of Science and Technology, Kochi - 682 022, India*
[$]*DRDO-Naval Physical and Oceanographic Laboratory, Thrikkakara, Kochi - 682 021, India*
[*]*E-mail: manojg.npol@gov.in*

ABSTRACT

We have proposed a new passive component-based coupling scheme to simultaneously transmit high power AC, high voltage DC and high speed data through a long, single core coaxial cable, particularly for Airborne Sonar applications. This method is intended to replace the bulky multicore cables with single core coaxial cables that are compact and effective for transmitting data over long distances. This coupling scheme consists of three couplers to superimpose high power AC, high voltage DC and high speed data at the onboard end of the cable, and three decouplers to separate them at the remote end. The long cable, couplers, decouplers and the acoustic transducer are represented by their corresponding equivalent circuits that are cascaded together to construct the complete network. Power loss in the circuit is minimised by providing impedance matching networks in the form of a T-network transmission line and a tuning coil. The Ethernet over Coaxial (EoC) module can transmit high speed Ethernet data at the rate of 10/100 Mbps for telemetry from onboard to remote units and vice versa. DC voltages up to 300 V are coupled to the single core coaxial cable from the onboard unit and superimposed with high power AC signals and high-speed data. Passive filter-based coupling and decoupling schemes are demonstrated. Network simulation studies and experimental studies are carried out to verify and validate the equivalent circuit model. The transfer functions of each set of couplers and decouplers are determined independently as well as collectively and their effects on the underwater acoustic performance of the system are studied. The model resuls are found to agree with experiments. The proposed system is capable of generating an acoustic Source Level of about 195 dB with the supply of 125 V continuous wave (CW) AC signals, with simultaneous transmission of data at 10 Mbps and DC supply of 260 V from the on-board unit to the remote unit at the end of a coaxial cable of 200 m length. Introduction of impedance matching network is found to increase the source level by about 12 dB.

Keywords: Equivalent circuit; Impedance matching; Underwater acoustic transducer; AC DC coupling; Data telemetry; EoC

1. INTRODUCTION

In data and high voltage AC power line communications, coupling schemes based on passive components are widely used[1] . Passive couplers combine different types of signals and filter out the frequenceis beyond the band of interest. Such schemes can be used to superimpose Ethernet over Coaxial (EoC) communication data with high voltage DC and high power AC signals over long cables. The coupling scheme has wide applications in airborne telemetry[2], high-frequency sonar telemetry[3], underwater modem, underwater communications and active sonobuoy. Multicore cable telemetries are commonly used in all these applications, which could be more economical, but have several engineering challenges. The multicore cable must be replaced with a single core coaxial cable, which requires all three signals to be coupled together using credible coupling schemes. The two types of coupling schemes that can be used in airborne sonars are relay-based and passive filter-based coupling[4-5]. High-speed data, DC voltage, and high-power AC are to be superimposed with the help of coupling and decoupling networks placed at the onboard and at remote end of the single-core coaxial cable, respectively. The challenges in the coupling schemes are discussed in the paper by Manoj[5], *et al.* A passive coaxial cable coupling scheme is proposed in this work for single-core telemetry between the onboard and remote units. The details of the equivalent circuit analysis, network simulation studies and experimental validation are presented in this paper.

Received : 30 August 2022, Revised : 09 March 2023
Accepted : 16 March 2023, Online published : 12 May 2023

2. COUPLING AND DECOUPLING SCHEMES

For airborne sonar applications, signals like high-speed EoC data, high-power AC, and high-voltage DC are essential for its operation. High-power AC is used to transmit sound signals through underwater projectors. High voltage DC is used to deliver DC supply at the remote end. The echo received from the target at the remote end is communicated onboard through a high-speed EoC module, which converts Ethernet data to coaxial signals. Controls are also transmitted to the remote end from the onboard end through a high-speed EoC module. Since these signals are well-separated bands of frequencies; it is possible to couple and decouple using passive

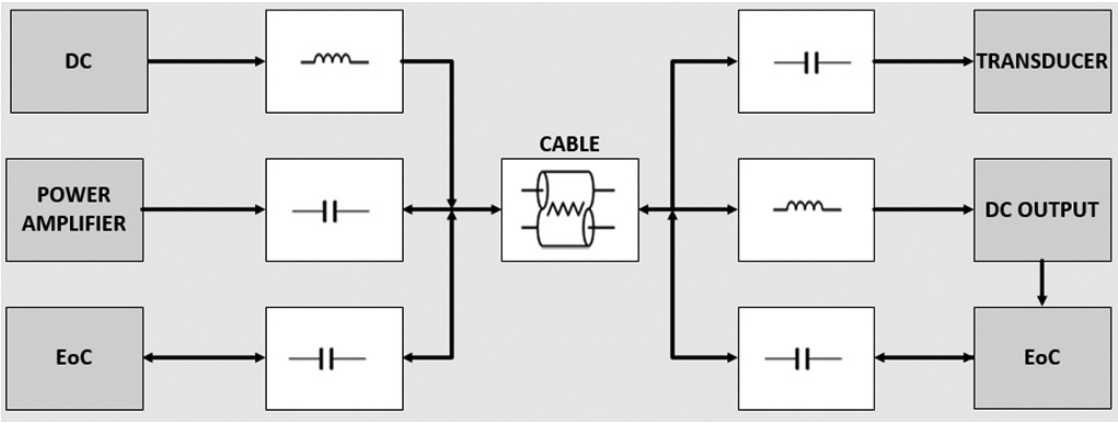

Figure 1. Block diagram of passive filter based coupling scheme.

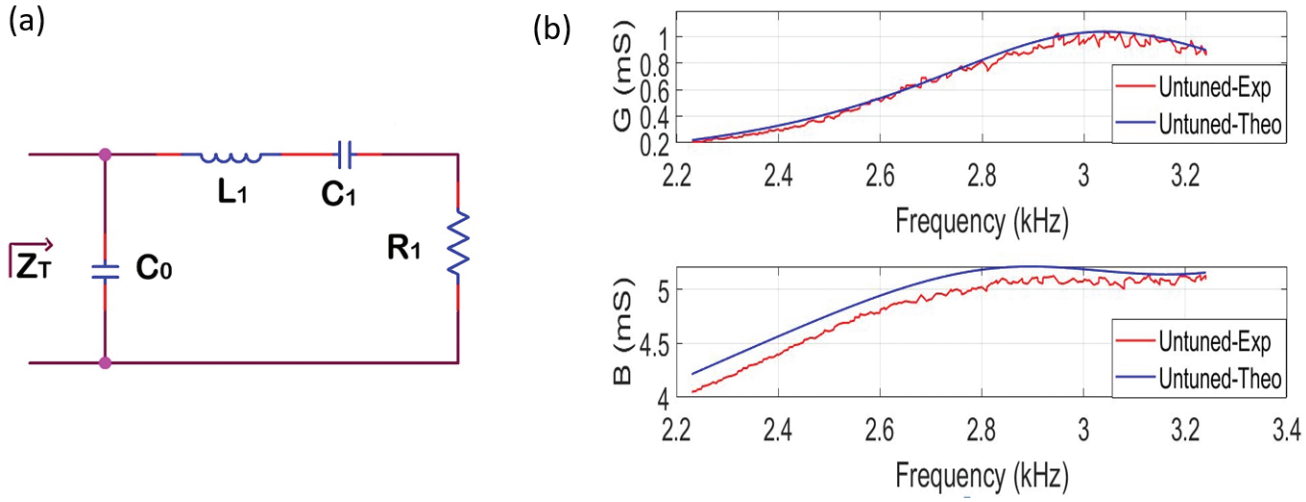

Figure 2. (a) Equivalent circuit of the underwater projector, and (b) Theoretical and measured electrical admittance plot of the bare underwater projector.

filters. Relay-based coupling scheme needs frequent switching of single-core coaxial cable to high power transmission and high-speed data as well as high voltage DC[5]. This scheme needs a DC source at the remote unit when the cable switches to high-power transmission. This issue is eliminated by using the passive filter-based coupling scheme.

A DC voltage of 300V is driven from the onboard end to the remote end of the cable in an airborne sonar application. Processed echo received from the remote end available in Ethernet form with a data rate of 10 Mbps is fed to the EoC module. The EoC module converts the Ethernet signals to coaxial cable signals and drives over the single-core coaxial cable. High-power AC signals of the range of 1kW are used for the active mode of operation of the airborne sonar. These signals are in well-separated band of frequencies and can be easily superimpose and separated with passive couplers and decouplers. Figure 1 shows the block diagram of the passive filter-based coupling scheme. At the onboard unit, passive couplers with inductor and capacitor are used to couple the high voltage DC, high power AC, and high-speed EoC data. Similarly, the signals are decoupled at the remote unit using an inductor and Capacitor filter.

3. EQUIVALENT CIRCUIT MODEL

The sonar transmitting system consists of an underwater electro-acoustic transducer positioned in the remote end of the system for generating acoustic signals in sea water. The transducer is electrically driven with a high power AC signal generated by a power amplifier positioned at the onboard end. Usually, long cables are used to connect the power amplifier to the transducer. This results in loss of power in the cable and needs to be compensated for. The PZT based transducer is an electromechanical system and cable is a purely electrical system. The combination of transducer and cable is in a mixed domain. Therefore, the transducer is represented by an equivalent electrical circuit[5] and the whole problem is analysed in the electrical domain by employing the well-developed electrical network theory.

3.1 Underwater Projector

Underwater transmitting transducers, known as a projectors, can be represented as a lumped-parameter electrical equivalent circuit[5] shown in Figure 2a. The parameters R_1, L_1 and C_1 are the electrical equivalents of the mechanical loss, mass and compliance, and C_0 is the dielectric capacitance of the piezoelectric transducer[5-7]. The electrical impedance of the Transducer Z_T is given by,

$$\frac{1}{Z_T} = Y_T = \frac{R_1}{R_1^2 + \left(\omega L_1 - \frac{1}{\omega C_1}\right)^2} + j\left[\omega C_0 - \frac{\left(\omega L_1 - \frac{1}{\omega C_1}\right)}{R_1^2 + \left(\omega L_1 - \frac{1}{\omega C_1}\right)^2}\right] = G + jB \quad (1)$$

The electrical admittance of the transducer in water is measured and used to determine the equivalent circuit parameters by implementing the method[7]. The equivalent circuit parameters of the projector selected for this study are given in Table. 1. The projector has a resonance frequency of 3000 Hz.

This correctness of the evaluated parameters is verified by plotting the theoretical conductance G and susceptance B with the measured data, as shown in Fig. 2(b). The close agreement validates the model and the method used in this analysis. Therefore, the transducer is replaced by the equivalent circuit shown in Fig. 2(a) with component values given in Table 1 and is cascaded with other components, such as, cable, tuning coil, matching layer and various couplers and decouplers, in the network for subsequent analysis.

Table 1. Equivalent circuit parameters of the transducer

Parameters	Values
$C_0(nF)$	56.50
$R_1(k\Omega)$	1.63
$L_1(H)$	0.21
$C_1(nF)$	6.11

3.2 Long Cable

For airborne sonar applications, projectors are often connected to the power amplifier through long cables. This introduces power loss and degradation in the system performance. In the present study, single-core coaxial cables are used and its electrical resistance and capacitance play a significant role. A long single-core coaxial cable is considered as a Transmission Line (TL)[8] as shown in Fig. 3. L_C, C_C, R_C and G_C are the inductance, capacitance, resistance and conductance per unit length of the cable.

These cable parameters are determined by measuring two sets of impedances at one end of the cable by keeping the other end open and short conditions successively. The corresponding impedances in these two cases are Z_1 and Z_2 respectively. The characteristics impedance (Z_0^C) and the propagation constant (γ^c) of the single core coaxial cable are calculated using the relations $Z_0^C = \sqrt{\frac{Z_2}{Z_1}}$ and $\gamma^C = \sqrt{Z_1 Z_2}$ [8]. The cable parameters per unit length are determined from these relations for a JDR brand single-core coaxial cable of 200 m and are given in Table. 2.

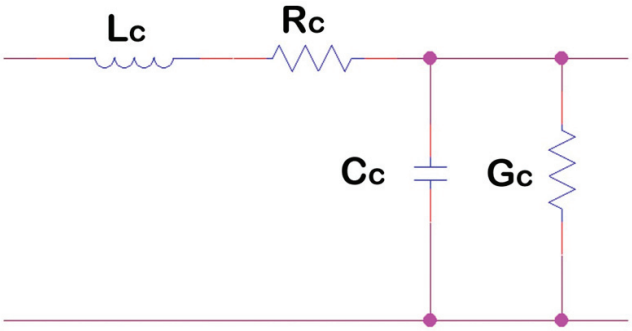

Figure 3. Equivalent circuit of the single core coaxial cable.

The characteristic impedance (Z_0^C) and phase velocity (υ_p) of the cable are related to the inductance (L_c) and capacitance (C_c) by,

$$Z_0^C = \sqrt{\frac{L_C}{C_C}} \quad (2)$$

$$\upsilon_p = \frac{1}{\sqrt{L_C C_C}} \quad (3)$$

The values of Z_0^C and υ_p of the cable used in the present study are determined as 57 Ohm and 1.78×10^8 m/s respectively.

Table 2. Chareacteristics of the JDR cable used in the present study

Length	Resistance (R_c)	Inductance (L_c)	Capacitance (C_c)	Conductance (G_c)
200 m	21.44 Ω	64 µH	19.7 nF	2.5 µS

4. TUNING COIL AND MATCHING LINE

Power loss occurs in the system due to impedance mismatch between the transducer and the long cable. First, the transducer is electrically tuned to nullify the effect of inherent capacitive reactance by using a Tuning Coil (TC). The resulting impedance is further matched with the characteristic impedance of the cable by using a Matching Line (ML). The design of the tuning coil and matching line are described in this section.

4.1 Design of Tuning Coil

A piezoceremic transducer is a capacitive device and its input impedance is reactive in nature, which accounts for significant power loss in the system. Therefore, the Power Factor (PF) is much less than unity, which is undesirable and has to be minimised. The capacitive reactance of the piezo ceramic transducer is tuned out by connecting a shunt inductor[6], whose value is determined from,

$$L_{TC} = \frac{1}{C_0 \omega^2} \quad (4)$$

The tuned transducer presents a purely resistive load to the power amplifier so that $Z_T = R_T$ at resonance. The equivalent circuit of the underwater projector with a tuning coil is shown in Fig. 4. The tuned transducer is electrically driven by a power amplifier. The input impedance of the tuned transducer (Z_{TT}) , as seen by the power amplifier, is,

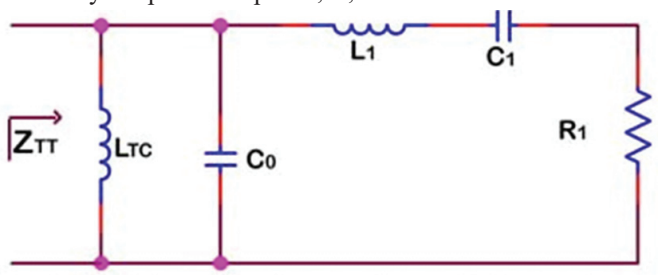

Figure 4. Equivalent circuit of the underwater projector with tuning coil.

$$Z_{TT} = \frac{Z_{p1} Z_T}{Z_{p1} + Z_T} \tag{5}$$

where,

$Z_T = Z_{L_1} + Z_{C1} + R_1$, $Z_{p1} = \frac{Z_{L_{TC}} Z_{C_0}}{Z_{L_{TC}} + Z_{C_0}}$, $Z_{L_{TC}} = j\omega L_{TC}$, $Z_{C_0} = \frac{1}{j\omega C_0}$

4.2 Design of Matching Line

Impedance mismatch and power loss are inevitable when a long, single-core coaxial cable is connected between the power amplifier and the tuned transducer[9]. To replace the multicore cable with a single-core coaxial cable, the high-power AC signal, high-speed data, and high-voltage DC must be transmitted simultaneously. The high-speed data and DC through the cable are decoupled from the high-power AC signals using a set of couplers and decouplers. The addition of reactive components, such as capacitors and inductors for creating coupler and decoupler circuits, introduces an additional impedance mismatch in the network. Therefore, it is essential to compensate for the imbalances caused by (i) the long cable, (ii) the AC coupler, (iii) the DC coupler, and (iv) the data coupler by designing an impedance matching network[10-13]. Figure 5 shows a T network[14] matching line implemented to match the cable impedance.

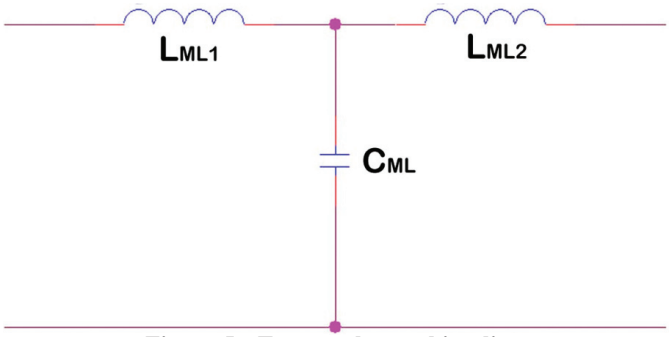

Figure 5. T network matching line.

The impedance of the tuned Transducer (Z_{TT}), given in Eqn. (5), is matched with the impedance of the cable (Z_{cable}) given by,

$$Z_{cable} = \frac{Z_{C_C} R_C + Z_{C_C} Z_{L_C}}{R_C + Z_{C_C} + Z_{L_C}} \tag{6}$$

The characteristic impedance of the matching line is determined by applying the principles of a quarter-wavelength transmission line[6]. Therefore,

$$Z_{ML} = \sqrt{Z_{cable} Z_{TT}} \tag{7}$$

The length of the quarter wavelength Matching Line (ML) corresponding to the phase velocity of 1.78 X 10^8 m/s and 3 kHz is about 15 km, which is impossible to implement in practice. Therefore, a matching line with equivalent characteristics is synthesized using a T-network of inductors. The symmetric T-network consists of two inductors L_{ML1} & L_{ML2} and capacitor, C_{ML} as shown in Fig. 5. The values of the inductor and capacitor per unit length are determined the characteristic impedance and phase velocity using the relations,

$$L_{ML} = \frac{Z_{ML}}{\upsilon_p} \tag{8a}$$

$$C_{ML} = \frac{1}{Z_{ML} \upsilon_p} \tag{8b}$$

5. THEORETICAL ANALYSIS OF PASSIVE FILTER COUPLER

This section discusses about the theoretical analysis on the effect of passive couplers and decouplers. Figure 6 shows the passive coupler and decoupler network diagram, which is connected between the onboard and remote units through a single-core coaxial cable. The onboard unit consists of AC coupler, DC coupler and Data coupler identified by the subscripts 1,2,and 3, respectively. The parameters corresponding to the onboard unit are identified by the subcript 'o'. Here V_1, V_2 are the voltage source across the AC coupler and DC coupler, while V_3 and V_4 are the voltage source across the coupler for high-speed EoC data at onboard and remote sides, respectively. Let C_{3o}, C_{4o}, C_{3r} and C_{4r} be the coupling capacitors to couple and decouple high-speed EoC data. L_{1o}, L_{2o}, L_{1r} and L_{2o} be are the coupling inductors to couple and decouple the DC. CC1*o*, CC2*o*, CC1*r* and CC2*r* are the coupling capacitors used to couple and decouple the high-power AC.

The onboard and remote unit are connected through a single-core coaxial cable. The parameters of the single-core coaxial cable include C_c, L_c and R_c. At the remote unit, the high-power AC decoupler is connected to the projector through a matching line and tuning coil LTC. The matching line is modelled with the T network mentioned in section 4, and the projector is modelled with an equivalent circuit, as discussed in section 3.

5.1 Power and Transfer Function of the AC Coupler

In order to determine the total power at the input of the power amplifier, all the voltage sources with load resistance except V_1 of Fig. 6, are replaced with load resistances at both onboard and remote units. Let R_{1o} and R_{2o} be the resistive load across high-voltage DC and high-speed EoC data onboard. Similarly, R_{1r} and R_{2r} are the resistive loads for high-voltage DC and high-speed EoC data at the remote unit.

Figure 7 is the network diagram where all the components are replaced with corresponding impedances. The total impedance of the circuit as seen by the power amplifier is calculated. Here Za is the parallel combination of C_{3o} and L_{1o} and *Zb* is the parallel combination of CC2*o*, L_{2o} and C_{4o}. Similarly, on the remote side, *Zc* and *Zd* are DC decoupler and data decoupler paths, respectively. The constant *Ze* is the parallel combination of C_c, *c* and *d*, where *c* and *d* are the DC and data decoupler paths, respectively.

$$Za = \frac{(Z_{L_{1o}} + R_{1o})(Z_{C_{3o}} + R_{2o})}{Z_{L_{1o}} + R_{1o} + Z_{C_{3o}} + R_{2o}} \tag{9a}$$

$$Zb = \frac{Z_{CC2o} Z_{L_{2o}} Z_{C_{4o}}}{Z_{CC2o} Z_{L_{2o}} + Z_{L_{2o}} Z_{C_{4o}} + Z_{CC2o} Z_{C_{4o}}} \tag{9b}$$

$$Zc = Z_{L_{1r}} + Z_{L_{2r}} + \frac{Z_{C_{1r}} R_{1r}}{Z_{C_{1r}} + R_{1r}} \tag{9c}$$

$$Zd = Z_{C_{3r}} + Z_{C_{4r}} + \frac{Z_{L_{3r}} R_{2r}}{Z_{L_{3r}} + R_{2r}} \tag{9d}$$

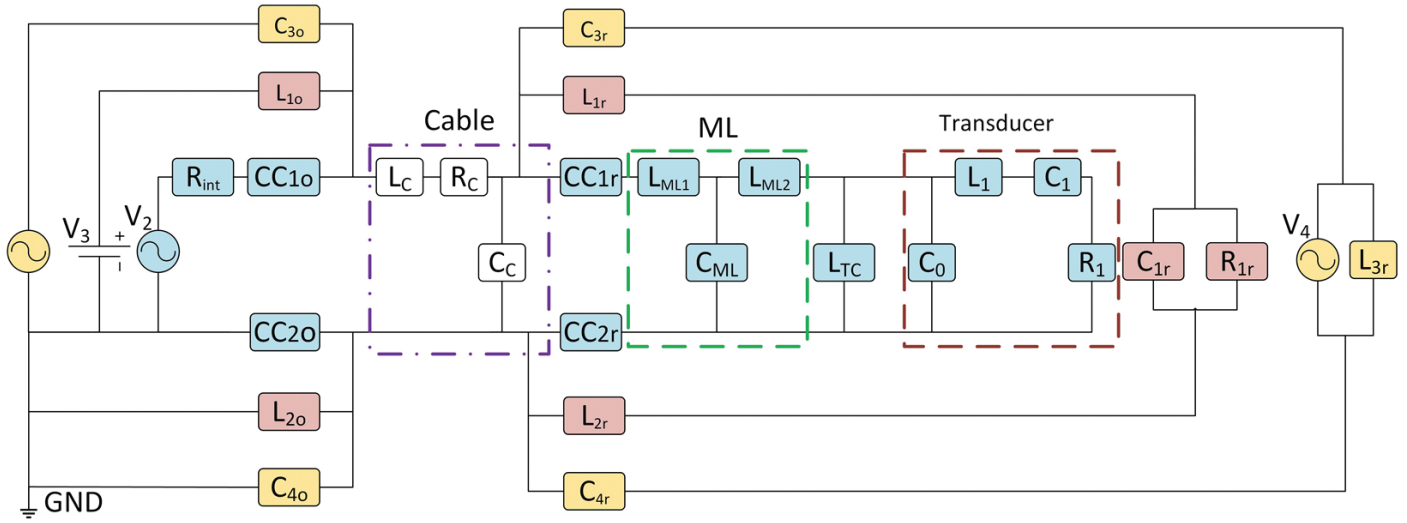

Figure 6. Network diagram of a passive coupler/decoupler. The subscripts 'o' and 'r' indicate onboard and remote units. The portions of the network corresponding to the cable, matching line and transducer are identified by dashed line boxes.

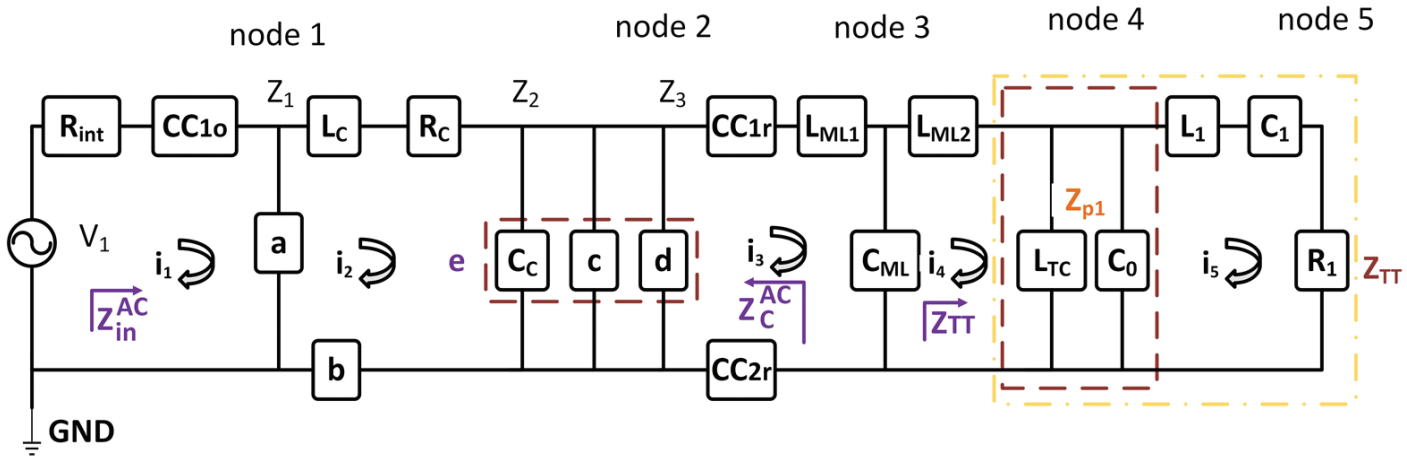

Figure 7. Simplified network diagram of passive coupler for AC analysis.

$$Ze = \frac{ZcZdZ_{C_C}}{ZcZd + ZdZ_{C_C} + ZcZ_{C_C}} \tag{9e}$$

The input impedance of the circuit with AC coupler as seen by the power amplifier is given by,

$$Z_{in}^{AC} = R_{\text{int}} + Z_{CC1o} + \frac{ZaZ_3}{Za + Z_3} \tag{10}$$

where,

$Z_1 = Z_{L_{ML2}} + \frac{Z_{p1}Z_T}{Z_{p1} + Z_T}$, $Z_2 = Z_{CC1r} + Z_{CC2r} + Z_{L_{ML1}} + \frac{Z_{C_{ML1}}Z_1}{Z_{C_{ML1}} + Z_1}$

$Z_3 = ZL_C + R_C + Zb + \frac{ZeZ_2}{Ze + Z_2}$ and Z_{p1}, Z_T and Z_{TT} are obtained from Eqn. (5).

$$\begin{bmatrix} x1 & -Za & 0 & 0 & 0 \\ -Za & x2 & -Ze & 0 & 0 \\ 0 & -Ze & x3 & -Z_{C_{ML}} & 0 \\ 0 & 0 & -Z_{C_{ML}} & x4 & -Z_{p1} \\ 0 & 0 & 0 & -Z_{p1} & x5 \end{bmatrix} \begin{bmatrix} i_1 \\ i_2 \\ i_3 \\ i_4 \\ i_5 \end{bmatrix} = \begin{bmatrix} V_1 \\ 0 \\ 0 \\ 0 \\ 0 \end{bmatrix} \tag{11}$$

where, $x1 = R_{\text{int}} + Z_{CC1o} + Za$, $x1 = Za + Zb + Z_{L_C} + R_C + Ze$,

$x3 = Ze + Z_{CC1r} + Z_{L_{ML1}} + Z_{CC2r} + Z_{C_{ML}}$, $x4 = Z_{C_{ML}} + Z_{L_{ML2}} + Z_{p1}$

and $x5 = Z_{p1} + Z_{L_1} + Z_{C_1} + R_1$

The current i_5 passing through loop 5 can be determined by solving equation (11). The electrical power delivered across the load resistance R_1 is converted useful acosutic power. It is obtained from the current $i_5 i_5$ and the voltage across R_1 (V_{out}^{R1}).

The current i_5 at passing through loop 5 can be determined by solving equation (11). The electrical power delivered across the load resistance R_1 is converted useful acosutic power. It is obtained from the current i_5 and the voltage across R_1 (V_{out}^{R1}).

$$V_{out}^{R1} = i_5 R_1 \tag{12}$$

A power amplifier supplies an RMS voltage of V_1 drives the circuit shown in Fig. 7 at their respective Node 1. The input impedance Z_{in}^{AC} is the load that the power amplifier experience. Therefore, the input electrical power drawn by the respective circuit is given by,

$$P_{in}^{AC} = \frac{V_1^2}{Z_{in}^{AC}} \tag{13}$$

The transfer function of the circuit is the ratio of the output voltage across R_1 to the input voltage supplied by the power amplifier. Therefore,

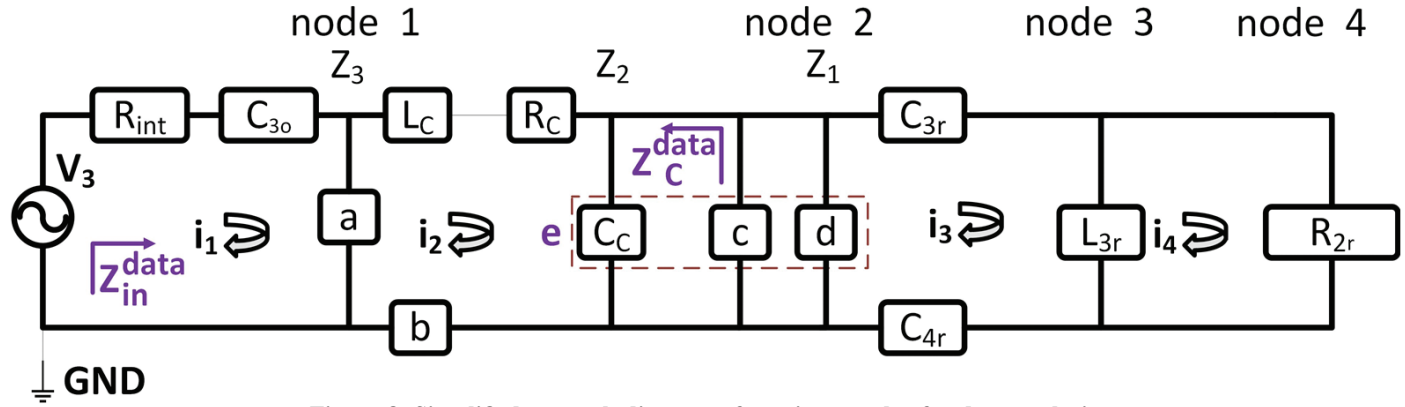

Figure 8. Simplified network diagram of passive coupler for data analysis.

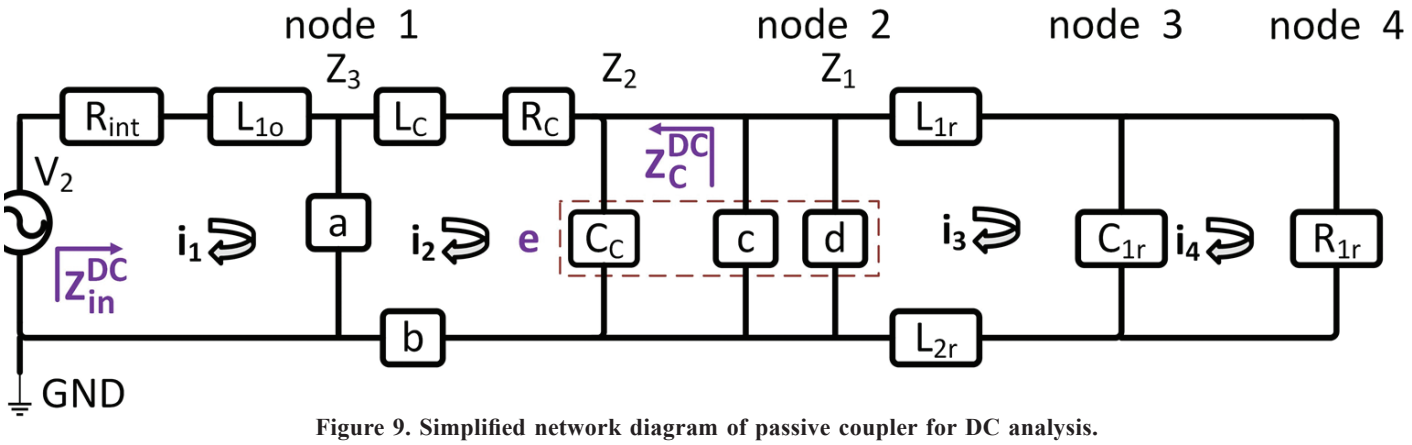

Figure 9. Simplified network diagram of passive coupler for DC analysis.

$$H(s)=\frac{V_{out}^{R1}}{V_1} \tag{14}$$

5.2 Transfer Function of the Data Coupler

The total power across the projector with data coupler in the circuit is determined in the next step. Let R_{1o} and R_{3o} be the resistive loads across high-voltage DC and high-speed EoC data onboard units. Similarly, R_{1r} and R_{2r} are the resistive loads for high-voltage DC and high-speed EoC data at the remote unit. Figure 8 is the network diagram to analyse the Data coupler. Here Za is the parallel combination of $CC1o$ and L_{1o} with the respective load resistors R_{1o} and R_{3o}, and Zc is the simplified equation of the AC decoupler.

$$Za=\frac{(Z_{L_{1o}}+R_{1o})(Z_{CC1o}+R_{3o})}{Z_{L_{1o}}+R_{1o}+Z_{CC1o}+R_{3o}} \tag{15a}$$

$$Zc=Z_{CC1r}+Z_{L_{ML1}}+Z_{CC2r}+\frac{(Z_{L_{ML2}}+Z_{TT})Z_{C_{ML}}}{Z_{L_{ML2}}+Z_{TT}+Z_{C_{ML}}} \tag{15b}$$

$$Zd=Z_{L_{1r}}+Z_{L_{2r}}+\frac{Z_{C_{1r}}R_{1r}}{Z_{C_{1r}}+R_{1r}} \tag{15c}$$

$$Z_{in}^{data}=Z_{C_{3o}}+R_{\text{int}}+\frac{ZaZ_3}{Za+Z_3} \tag{16}$$

Where,

$$Z_1=Z_{C_{3r}}+Z_{C_{4r}}+\frac{Z_{L_{3r}}R_{2r}}{Z_{L_{3r}}+R_{2r}},\ Z_2=\frac{ZeZ_1}{Ze+Z_1},Z_3=Z_{L_c}+R_c+Z_2+Zb$$

and Zb & Ze is taken from Eqn. (9b) and (9e).

$$\begin{bmatrix} x_1 & -Za & 0 & 0 \\ -Za & x_2 & -Ze & 0 \\ 0 & -Ze & x_3 & -Z_{L_{3r}} \\ 0 & 0 & -Z_{L_{3r}} & x_4 \end{bmatrix}\begin{bmatrix} i_1 \\ i_2 \\ i_3 \\ i_4 \end{bmatrix}=\begin{bmatrix} V_3 \\ 0 \\ 0 \\ 0 \end{bmatrix} \tag{17}$$

Here,

$$x_1=R_{\text{int}}+Z_{C_{3o}}+Za\,,x_2=Za+Z_{L_c}+R_c+Ze+Zb\,,$$

$$x_3=Z_{C_{4r}}+Z_{L_{3r}}+Z_{C_{3r}}+Ze\ ,\ x_4=Z_{L_{3r}}+R_{2r}$$

Current i_4 for the network diagram shown in Fig. 8 is obtained by solving the matrix Eqn (17), and finally, the voltage across R_{2r} is calculated as:

$$V_{out}^{R2r}=i_4R_{2r} \tag{18}$$

Therefore the transfer function of the data coupler is

$$H(s)=\frac{V_{out}^{R_{2r}}}{V_3} \tag{19}$$

5.3 Transfer Function of the DC Coupler

The Transfer Function of the DC coupler is calculated after replacing all the Voltage sources with resistive load except V_2 in Fig. 6. Let R_{1o} and R_{3o} be the resistive load across high-voltage DC and high-speed EoC data onboard units. Similarly, R_{1r} and R_{2r} are the resistive loads for high-voltage DC and high-speed

EoC data at the remote unit. The simplified network diagram for analysis of the DC coupler is shown in Fig. 9.

$$Za = \frac{(Z_{CC1o} + R_{3o})(Z_{C_{3o}} + R_{2o})}{(Z_{CC1o} + R_{3o}) + (Z_{C_{3o}} + R_{2o}} \quad (20a)$$

$$Zc = Z_{CC1r} + Z_{L_{ML1}} + Z_{CC2r} + \frac{(Z_{L_{ML2}} + Z_{TT})Z_{C_{ML}}}{Z_{L_{ML2}} + Z_{TT} + Z_{C_{ML}}} \quad (20b)$$

Where, Z_T, Z_{P1} and Z_{TT} are taken from Eqn. (5)

$$Zd = Z_{C_{3r}} + Z_{C_{4r}} + \frac{Z_{L_{3r}} R_{2r}}{Z_{L_{3r}} + R_{2r}} \quad (20c)$$

$$Z_{in}^{DC} = R_{\text{int}} + Z_{L_{1o}} + \frac{Z_a Z_3}{Z_a + Z_3} \quad (21)$$

Where $Z_1 = Z_{L_{1r}} + Z_{L_{2r}} + \frac{Z_{C_{1r}} R_{1r}}{Z_{C_{1r}} + R_{1r}}$, $Z_2 = \frac{ZeZ_1}{Ze + Z_1}$

and $Z_3 = Z_{L_c} + R_c + Z_2 + Z_b$.

The values of *Zb* and *Ze* is taken from Eqn. (9b) and (9e).

$$\begin{bmatrix} x_1 & -Za & 0 & 0 \\ -Za & x_2 & -Ze & 0 \\ 0 & -Ze & x_3 & -Z_{C_{1r}} \\ 0 & 0 & -Z_{C_{1r}} & x_4 \end{bmatrix} \begin{bmatrix} i_1 \\ i_2 \\ i_3 \\ i_4 \end{bmatrix} = \begin{bmatrix} V_2 \\ 0 \\ 0 \\ 0 \end{bmatrix} \quad (22)$$

Where x_1, x_2, x_3 and x_4 are the variables used to simplify the matrix Eqn. (22).

$x_1 = R_{\text{int}} + Z_{L_{1o}} + Za$, $x_2 = Za + Z_{L_C} + R_C + Ze + Zb$,
$x_3 = Ze + Z_{L_{1r}} + Z_{L_{2r}} + Z_{C_{1r}}$ and $x_4 = Z_{C_{1r}} + R_{1r}$.

The current i_4 is calculated by soving Eqn. (22). The voltage across the load resistor R_{1r} is calculated as

$$V_{out}^{R1r} = i_4 R_{1r} \quad (23)$$

Therefore the transfer function of the DC coupler is

$$H(s) = \frac{V_{out}^{R1r}}{V_2} \quad (24)$$

6. SIMULATION ANALYSIS

Network simulations studies are carried out using Multisim Multisim to verify the theoretical results. Figure 10, shows the combined simulation circuit of the passive filter-based coupling and decoupling scheme for the single-core coaxial cable telemetry with the single-core coaxial cable model.

For applications like airborne sonar, the single-core coaxial cable should handle high-power AC, high-voltage DC, and high-speed data simultaneously. As the circuit deals with a high-power AC signal, it is essential to study the effect of high-power AC in other coupling paths, i.e., onboard data coupler, onboard DC coupler, remote DC coupler, and remote data coupler. The electrical power drawn by the circuits from the power amplifier for combined AC, DC, and Data coupler is predicted in this analysis. Theoretical analysis based on the equivalent circuit model described in section 5 is verified by simulation studies. The circuit design is carried out in Multisim 14. The frequency responses of each coupler are plotted. Simulations are carried out with a single-core coaxial cable model to find leakage of high voltage DC, high power AC and high-speed EoC data in each coupling path on both onboard and remote sides. The coaxial cable model is implemented based on the measured characteristics of the single-core coaxial cable.

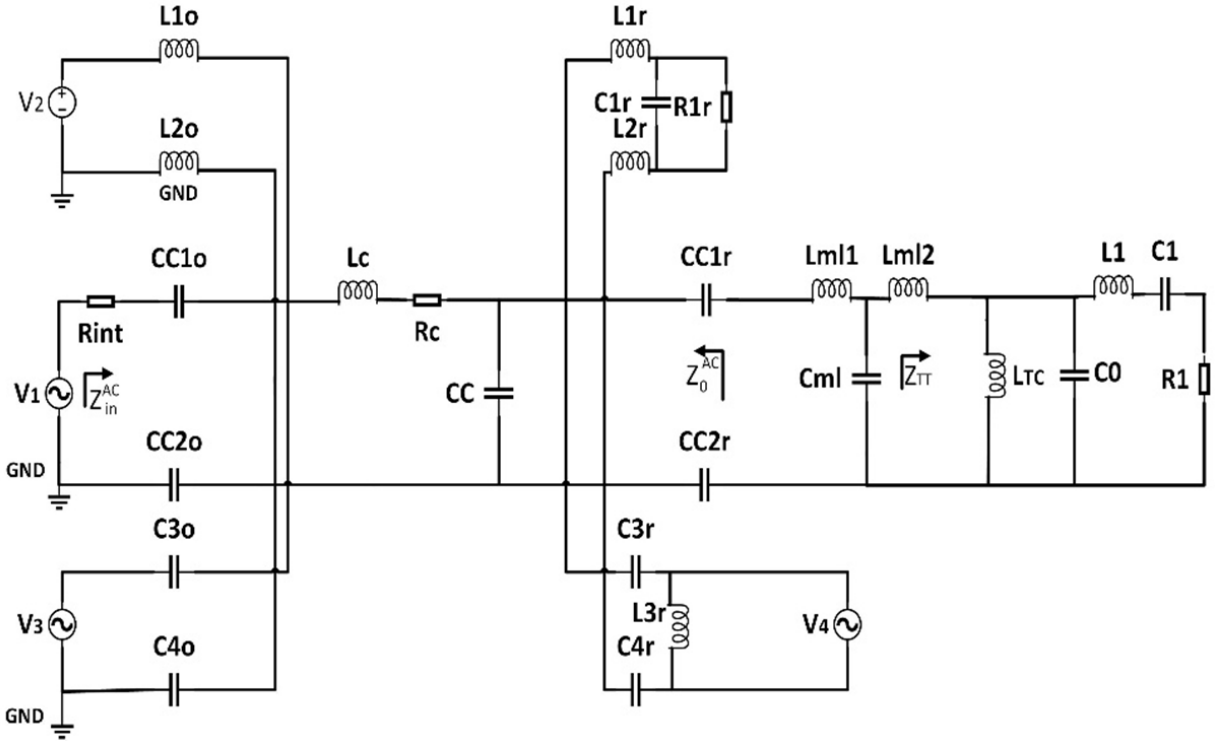

Figure 10. Simulation circuit diagram.

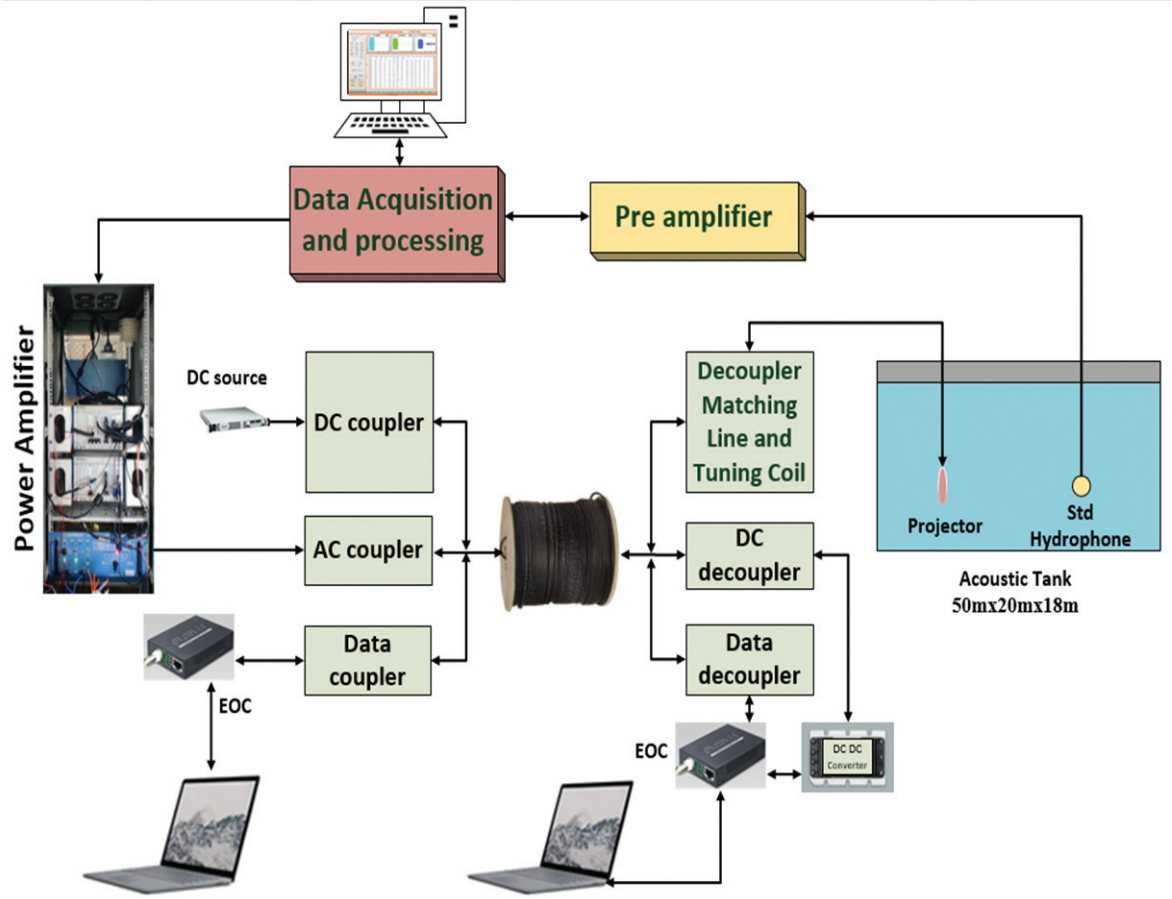

Figure 11. Experimental setup for measurement of high power AC transmission.

7. EXPERIMENTAL VALIDATION

We have conducted experiments to validate the modeled results. A prototype circuit with a Passive coupler and decoupler as shown in Fig. 10 is constructed. The characteristics of the coupler are measured using the experimental facility. The experimental setup consists of a transducer, tuning coil, matching lines, 200 m long cable, the couplers and decoupler, the data acquisition system, power amplifier, DC supply, and EoC modules shown in Fig. 11.

The experimental facility consists of an acoustic tank to study the high-power AC transmission. The test transducer and a standard hydrophone are positioned with a separation of 3 m at 6 m depth. The transducer is connected to the power amplifier (Make: Instruments Inc, Model: L10) through the tuning coil, matching line, 200 m long cable, and the respective couplers (AC, DC, and Data) at the remote unit. The signal for high-power transmission is generated by the data acquisition and processing system and fed to the power amplifier. The high-power signal is decoupled from the high-voltage AC Decoupler at the remote end of the cable. The standard hydrophone is connected to the data acquisition and processing unit (NI and LabView) through a preamplifier (B&K Nexus). The input electrical impedance spectra are determined from the voltage and current values of the transmitted signals. The Transmitting Voltage Response (TVR) and Source Level (SL) of the Transducer with all associated circuits are measured using the setup shown in Fig. 11. The voltage at the output of the amplifier is maintained constant at 125 Vrms throughout the band of interest. Input power is determined from the voltage and current outputs of the power amplifier that drives the circuits described in section 5.

The DC source is connected to the onboard unit to couple DC voltage to the cable and decouples at the remote unit. The DC Decoupler output is fed to a DC-DC converter to source the power at the remote unit electronics. Similarly, the Ethernet data generated from a laptop is considered as the data to be transmitted through the single-core coaxial cable. The Ethernet data is fed to the EoC module, which will convert Ethernet to a Coaxial signal. The output of the EoC at the onboard unit is connected to the remote unit Data coupler through a single-core coaxial cable. The Decoupler output is connected to the EoC, which converts back to Ethernet.

8. RESULTS AND DISCUSSIONS

8.1 Transfer Function of AC, DC, and Data Couplers

The transfer function of a circuit is a measure of the effectiveness with which the circuit transfers the data through it with minimum loss of signal. The transfer functions of various circuits described in section 5 are predicted by the theoretical studies and validated by experiments. Fig. 12 shows the transfer function of a high-power AC coupler, high-voltage DC coupler, and high-speed data coupler. The plots are obtained from the ratio of the output voltage to input voltage in each case. Figure

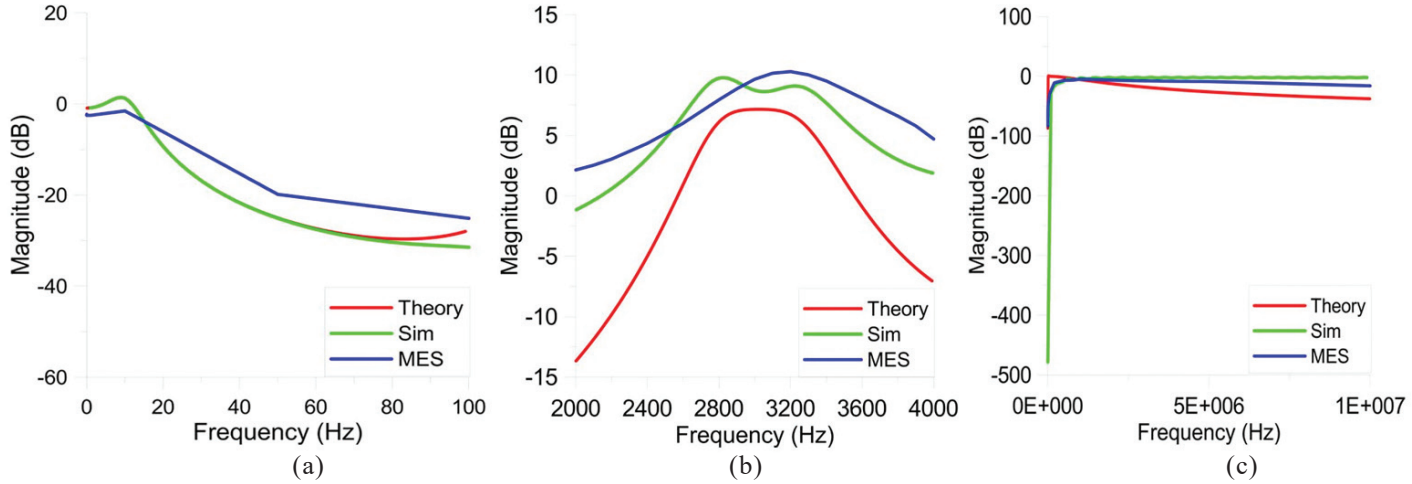

Figure 12. Transfer Function of (a) DC coupler, (b) AC coupler, and (c) Data coupler.

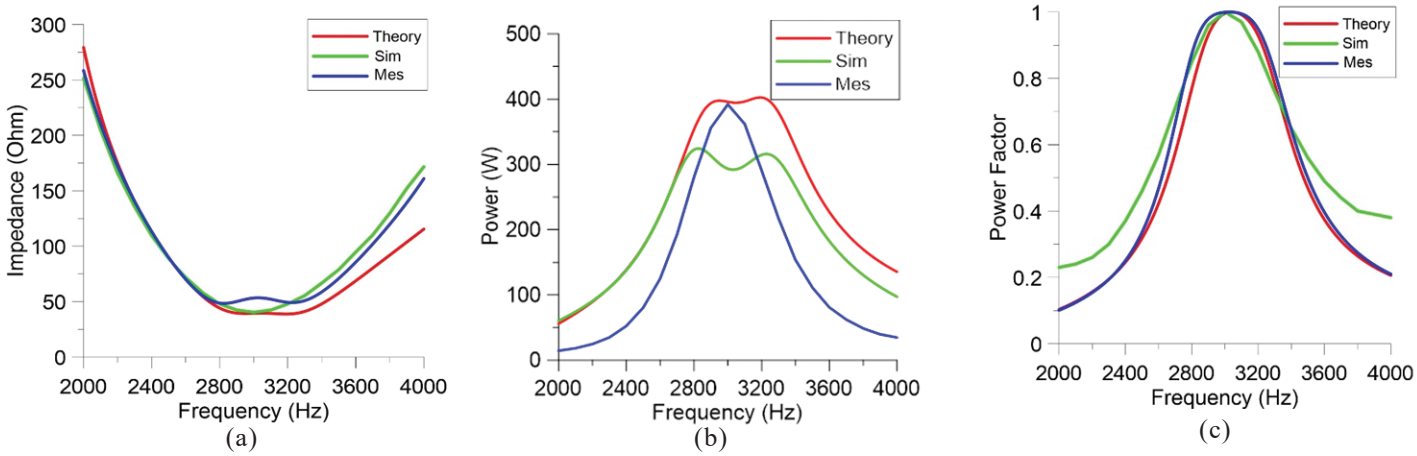

Figure 13. (a) Impedance, (b) Power and (c) Power factor.

12(a) shows the low pass response of the DC coupler, where a frequency below 20 Hz will pass through the coupler along the cable. The DC is entirely blocked at the AC coupler with more than -150 dB components. Figure 12(b) is the transfer function of the AC coupler measured across the output of the AC coupler to the input. Here the coupler is a high pass in nature, but the response is a band pass due to the behavior of the transducer. At lower and higher frequencies below 2000 Hz and above 4000 Hz, the signals are attenuated more than 8 dB. The resonance occurs within the bands of 2000 Hz and 4000 Hz as the peak is obtained at 3000 Hz.

The signals up to 500 kHz were blocked at the Data coupler, shown in Fig. 12(c). At low frequencies, attenuations of DC come around -300 dB, which explains that DC is completely blocked at this coupler. In all the figures, the measured results of all the couplers are well within the limit of theoretical and simulation results.

8.2 Impedance, Power, and Power Factor

The theoretical model calculates the circuit's power, input impedance and power factor for the AC coupler. Fig. 13 is the comparison of theoretical results with the results of Multism simulation studies and experimental data. The input impedane of the circuit with AC coupler $\left(Z_{in}^{AC}\right)$ is the load impedance to the power amplifier and is determined from Eqn. (12) at node 1 of Fig. 7. The measured impedance seen by the power amplifier is 40 ohms at the resonance frequency of 3000 Hz. The impedance for simulation and measurement is approximately 40 ohms and 55 ohms at a resonance of 3000 Hz. Comparative plots of impedance are shown in Figure 13(a).

Figure 13(b) is the comparison of power spectrum determined by equivalent circuit model, network simulation stuides and measurements in an acoustic tank The power predicted by the theoretical studies is 395 watts, which matches very well with the measured power of 392 watts at 3000 Hz, validating the equivalnet circuit model presented in this work. Also, the Power Factor comes close to unity at resonance in all the three results, as seen in Fig. 13(c).

8.3 Acoustic Response

Transmit voltage response (TVR) and Source level (SL) are the important acoustic characteristics of an underwater transducer[6]. TVR and SL of the transducer with impedance matching network and the DC, AC and Data coupleres and decouplers inlcuded in the circuit are experimentally measured in the measurement facility shown in Figure 11. The measured results are shown in Fig. 14. The uncerainty in acoustic mesuredments are estimated to be ± 1.5 dB. The peak TVR and

SL for transducer with matching line and tuning coil are found to be about 153 dB ref. µPa/V at 1 m and 195 dB ref. 1 µPa at 1m, respectivley, for an input voltage of 125 V. These values for the bare tranducer without impedance matching network is about 141 dB and 183 dB, respectively. This shows that cable matching has improved the performance and the addition of couplers in the circuit don't degrade the acoustic performance of the system.

8.4 Data Communication

The Ethernet over Coaxial (EoC) data to the single-core coaxial cable is realized through a high-frequency data coupler. The high-voltage DC should be available without loss at the remote unit throughout the operation. For sending data from a remote unit, a LabVIEW code was developed to generate digital samples of the sine wave. Here for testing purposes, 24 channel data are generated. On the onboard side, LabVIEW code for ethernet data reception is also developed. This data in ethernet format at the remote side is fed to the EoC module. The EoC module drives the Ethernet data to Coaxial signals, which are in analog form. On the remote side, the EoC module recovered the analog signal and converted it back in to Ethernet format. Two PCs were placed on both the onboard and the remote sides, and data was successfully transmitted across the 200m cable from the onboard unit to the remote unit and vice versa. Figure 15(a) shows the LabVIEW GUI snapshots for data generation.

The signal generator generates signals of any frequency up to 4 kHz, with an amplitude of 5 V. Provisions are given to switch off digital samples for corresponding channels. Figure 15(b) shows the Analog signal, spectrum, and intensity graph of 24-channel received signals. The signal that is generated from the remote side has only alternate channels and is received onboard with alternate channels without any degradation. The spectrum shows the exact 500 Hz signal. The spectrum and its sine waveform are also shown in Fig. 15(b). This indicates the faithfull reproduction of data through the Data coupler an decoupler implemented in the present method.

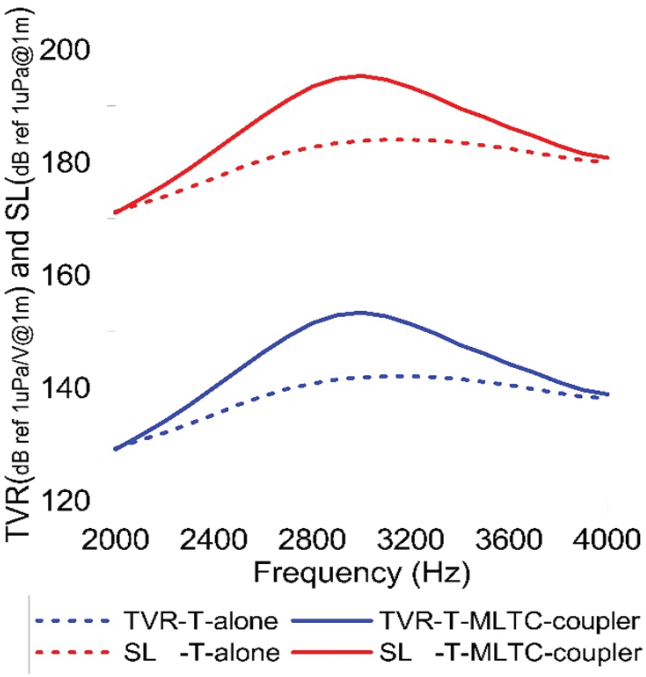

Figure 14. TVR and SL.

8.5 DC Measurement

Table 3 shows the component of DC at all the coupler outputs. From the measurement, it is clear that there is no DC component at the output of the onboard coupler, remote high-

Table 3. DC measurements across the coupler

Coupling	Voltage (V)
Onboard data coupler	0
Onboard DC coupler – Input	262
Remote data coupler	0
Remote DC coupler – output	150
Remote AC coupler	0

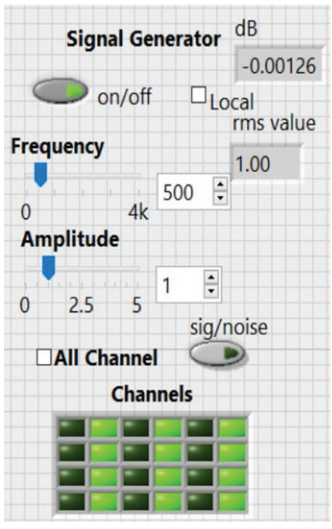

(a)

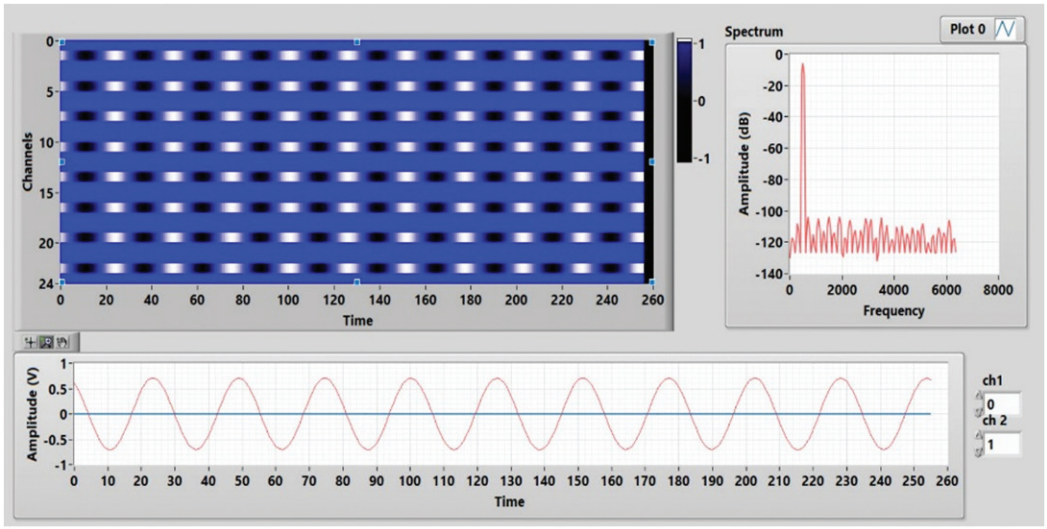

(b)

Figure 15. (a) Lab VIEW GUI to send 24 channel ethernet data, and (b) received data at the remote side.

speed data coupler, and high-power AC coupler. The insertion loss due to the DC coupler and the Data coupler introduces DC loss over the cable. A high-voltage DC supply is sent to the remote unit to manage the cable loss so that the required power supply is available at the remote unit. A DC-DC converters will help to develop the required DC to power up the remote side. electronics.

8. CONCLUSIONS

A passive filter-based scheme is proposed and demonstrated to simultaneoudly transmit high power AC, high voltage DC and high speed data through a single-core coaxial cable. High power signal transmission is essential to enable active mode of operation in airborne sonar. It is also essential to transmit sonar data and high voltage DC along with the AC signal. Ethernet over Coaxial (EoC) is standard telemetry technique commonly employed for sonar data transmission. Transmission of different types of signals, such as AC, DC and high-speed data, from the onboard end to the remote end is usually executed by using multicore cables with dedicated lines for each type of signals. This method results in a bulky system, and is un-desirable and impractical to implement is air-borne sonar systems where compactness is of prime importance. An alternative method which finds an effective solution to arrive at a compact system for air-borne sonar is demonstrated in this work.

Electrical equivalent circuit model is proposed to analyse the network that comprises of AC coupler, DC coupler, Data coupler, their corresponding de-couplers, long coaxial cable, tuning coil and underwater transducer. The underwater acoustic transducer is represented by its electrical equivalent circuit. The reactive impedance of the transducer is nullified by providing an electrical tuning network. In order to ensure lossless transmission through the long cable, T-network impedance matching scheme is implemented between the coaxial cable and the tuned transducer. The power amplifier that drives the network is considered as a voltage source with a series source resistance. The voltage transfer function and electrical power of the network with various coupling schemes dealing with AC, DC and Data couplers and decouplers are analysed theoretically. The model results are verified by carrying out network simulation studies using Multisim package and validated by experimental studies. It is found in this work that the model results agree well with the measured data validating the model.

Various coupling schemes, such as, AC coupling, DC coupling and Data coupling and their corresponding decoupling schemes are demonstrated by simultaneously transmitting high power AC sonar signal, high voltage DC supply and high speed data through EoC single-core coaxial cable of 200 m length. All the three types of signals are transmitted from the onboard end of the cable and faithfully reproduced at the remote end without loss of signal. The high-speed data and high-power AC are tested over the prototype board with a high voltage of 260 V DC. The Ethernet data is fed to the input of EoC at the onboard unit and converted back to coaxial data at the remote unit. High-speed data Telemetry through EoC over high-voltage DC is tested along with high-power AC, and the same is validated with measurement data. The DC at the remote end is found sufficient to generate the required power supply (+/- 5V and +/- 12V DC) at the remote unit.

The underwater acoustic characteristics, such as, Transmit voltage response (TVR) and Source level (SL) of the complete system are measured experimentally in an acoustic tank facility. The TVR and SL are found to be about 153 dB (ref. µPa/V at 1 m) and 195 dB (ref. 1µPa at 1m), respectivley, for an input voltage of 125 Vrms.

The implementation scheme of EoC cable telemetry over high power AC and high voltage DC through a long singl-core coaxial cable scheme is demonstrated and found useful for air-borne sonar applications where compactness is of prime importance.

REFERENCES

1. Luis Guilherme da S. Costa, Antonio Carlos M. de Queiroz, Bamidele Adebisi, Vinicius L. R. da Costa & Moises V. Ribeiro, Coupling for power line communication: A survey. *J. Commun. Inf. Syst.*, 2017, **32**(1). doi:10.14209/jcis.2017.2
2. J.E. Hardiman, T.N.; Rosario, T. Quellette & Hegg, F. High repetition rate side looking SONAR. *OCEANS* 02, **4**, 2268-2272. doi: 10.1109/OCEANS.2002. 1191983
3. Belcher, E.; Hanot, W. & Burch, J. Dual-frequency identification sonar (DIDSON). *In* International Symposium on Underwater Technology*,* 2002, pp. 187-192. doi: 10.1109/UT.2002.1002424
4. Manoj, G.; Jaco, E. & Kundukulam, S.O. Design, simulation, and comparison of mixing schemes for DC, AC, and bi-directional data through coaxial cable, *Procedia Comput. Sci.,* 2016, 578-584. doi:10.1016/j.procs.2016.07.303
5. Manoj, G.; Jacob, E. & Kundukulam, S.O. Relay-based coupling scheme of high-speed communication data, high voltage dc and high power pulsed ac for coaxial cable, *Def. Sci. J.,* 2018, 487-493. doi: 10.14429/dsj.68.11907
6. Rathod, V.T. A review of electric impedance matching techniques for piezoelectric sensors, actuators and transducers. *Electronics*, 2019 **8**, 169. doi:10.3390/electronics8020169
7. Radke. H.N. Development of a self-tuning amplifier for piezoelectric transducer evaluations. *Open Access Master's Theses.* Paper 80, 2013. doi:10.2386/thesis-radkr-hayden-2013.
8. Safari, A.E.; Koray, A., eds. Piezoelectric and acoustic materials for transducer applications*. Springer Sci. Business Media*, 2008. doi:10.1007/978-0-387-76540-2.
9. Q.Shi, Qinghai & Kanoun, Olfa. Analysis of the parameters of a lossy coaxial cable for cable fault detection, *Transact. Syst. Signals Devices*. 2012, **7**, 311-325. doi:10.1109/SSD.2011.5767393.
10. Zhou, Hanyun; Huang, S.H. & Li, Wei. Electrical impedance matching between piezoelectric transducer and power amplifier. *IEEE Sensors J.,* 2020.

doi:10.1109/JSEN.2020.3008762
11. Frederick, Ray & Gomez, I. Design of impedance matching networks for RF applications. *Asian J. Eng. Technol.,* 2018, **6**(4). doi:10.24203/ajet.v6i4.5450.
12. Taherinejad, N.; Lampe, L. & Mirabbasi, S. An adaptive impedance matching system for vehicular power line communication. *IEEE Trans. Veh. Technol.*, 2017, **66**(2), 927–940. doi:10.1109/ISPLC.2014.6812364.
13. Rodriguez., G.M.; García.Álvarez, J.; Yanez, Yasmin; Garcia.Hernandez, Miguel; Salazar, Jordi; Turo., A.; Domínguez, Chávez & Antonio, Juan. Low cost matching network for ultrasonic transducers. *Phy. Proc.,* 2010, **3**, 1025-1031. doi:10.1016/j.phpro.2010.01.132.
14. Bingting, Wang; Ziping, Cao & Song, Fei. Design and evaluation of a T-shaped adaptive impedance matching system for vehicular power line communication, *IEEE Access*, 2020. doi: 10.1109/ACCESS.2020.2988299,.

ACKNOWLEDGEMENT

The authors thank the Director, Naval Physical and Oceanographic Laboratory for permisson to carry out this work and publish this paper. The authors also thank Krishnakumar R. and Satheesh Kumar O.B. for their help in conducting acosutic measurements in tank facility.

CONTRIBUTORS

Mr Manoj G. obtained MSc in Physics from Kerala University and he has been working as a Scientist at DRDO-NPOL, Kochi. His research interests include the design and development of front-end hardware for airborne sonar and imaging sonar, airborne sonar telemetry, and RF systems for sonobuoy applications. In the current study he carried out the theoretical and simulation studies and the results were validated with measurment results conducted in tank experiments.

Dr R. Ramesh ontained his Ph.D. degree in 1994. He worked as a Post-Doctoral Fellow at IIT, Madras, and as Visiting Scientist with IGCAR, Kalpakkam. He is currently working with NPOL, Kochi. His current research interests include designing, modeling, and analysing piezoelectric transducers.
His contributions in this paper is to verify and validate the experimental results that conducted in tank experiments

Dr Sona O. Kundukulam obtained PhD (Microwave Electronics) Cochin University of Science & Technology, India. She is currently working as a Scientist at DRDO-NPOL, Kochi. Her areas of interest include: working on designing and developing RF systems for airborne sonars.
Her contrinbutions in this paper is to verify the results with respect to simulation and theoretical analysis.